Electronic Supplementary Material (ESI) for Catalysis Science & Technology.
This journal is © The Royal Society of Chemistry 2021

Electronic Supplementary Information (ESI) for

Deposition of Highly Dispersed Gold Nanoparticles onto Metal Phosphates by Deposition-Precipitation with Aqueous Ammonia

Hidenori Nishio,[a] Hiroki Miura,[a,b,c*] Keigo Kamata[d] and Tetsuya Shishido[a,b,c,e*]

[a] Department of Applied Chemistry for Environment, Graduate School of Urban Environmental Sciences, Tokyo Metropolitan University, 1-1 Minami-Osawa, Hachioji, Tokyo 192-0397, Japan

[b] Research Center for Hydrogen Energy-based Society, Tokyo Metropolitan University, 1-1 Minami-Osawa, Hachioji, Tokyo 192-0397, Japan

[c] Elements Strategy Initiative for Catalysts & Batteries, Kyoto University, Katsura, Nishikyo-ku, Kyoto 615-8520, Japan

[d] Laboratory for Materials and Structures, Institute of Innovative Research, Tokyo Institute of Technology, Nagatsuta-cho 4259, Midori-ku, Yokohama-city, Kanagawa, 226-8503, Japan.

[e] Research Center for Gold Chemistry, Tokyo Metropolitan University, 1-1 Minami-Osawa, Hachioji, Tokyo 192-0397, Japan

* Corresponding author: Tel: +81-42-677-2850 Fax: +81-42-677-2821 (H. Miura, T. Shishido)

E-mail address: miura-hiroki@tmu.ac.jp (H. Miura)

E-mail address: shishido-tetsuya@tmu.ac.jp (T. Shishido)

Analytical data

Contents:

1. Point of zero charge (PZC) of supports.

Table S1 PZC of supports

Support	PZC
$GaPO_4$	3.4 - 4.5
$AlPO_4$	3.9 - 4.5
ZrP_2O_7	1.9 - 2.8
$CrPO_4$	1.2 - 4.2
HAP	2.6 - 3.1
YPO_4	3.2 - 3.5
$Zn_2P_2O_7$	< 1.3
$CePO_4$	4.3 - 5.0
TiO_2	5.0 - 6.5
Y_2O_3	7.8 - 8.9
Ga_2O_3	6.4 - 8.3
ZrO_2	7.3 - 9.7
Al_2O_3	8.7 - 9.2

2. XRD patterns of supported Au catalysts.

2-1. XRD patterns of Au/ZrP_2O_7 prepared by different preparation methods.

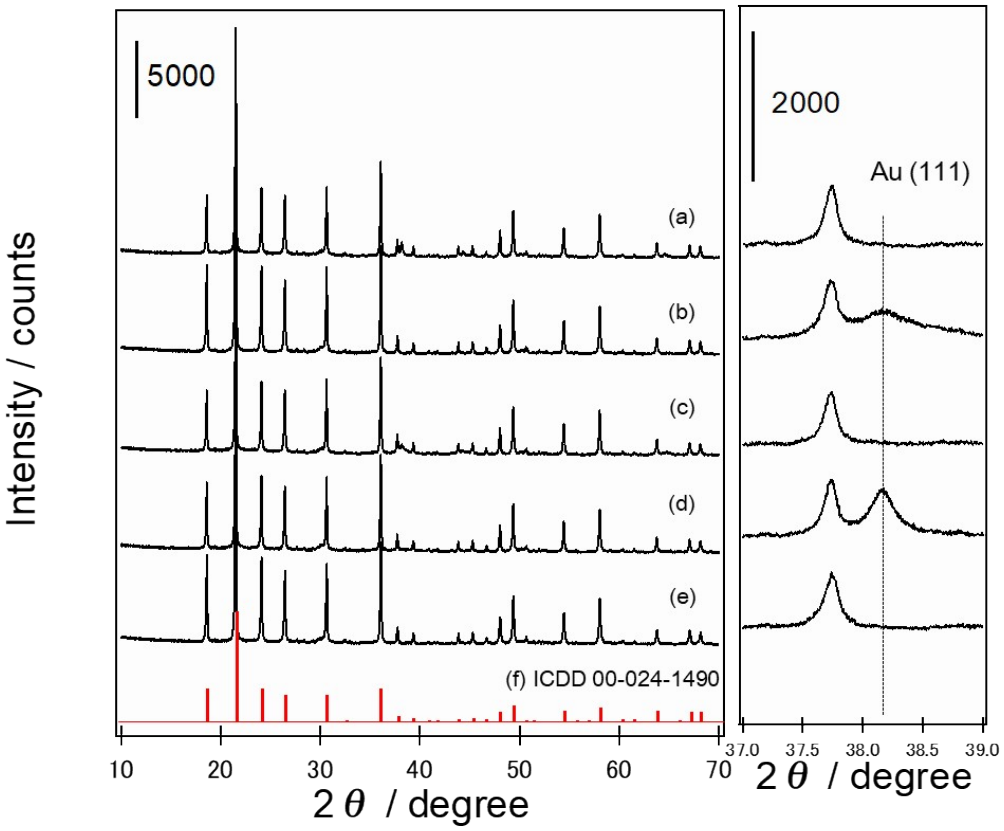

Fig. S1 XRD patterns of Au/ZrP_2O_7 prepared by different preparation methods (a) DPNa, (b) DPU, (c) DPA, (d) DPen, and (e) ZrP_2O_7 and (f) the reference information.

2-2. XRD patterns of metal phosphate-supported Au catalysts.

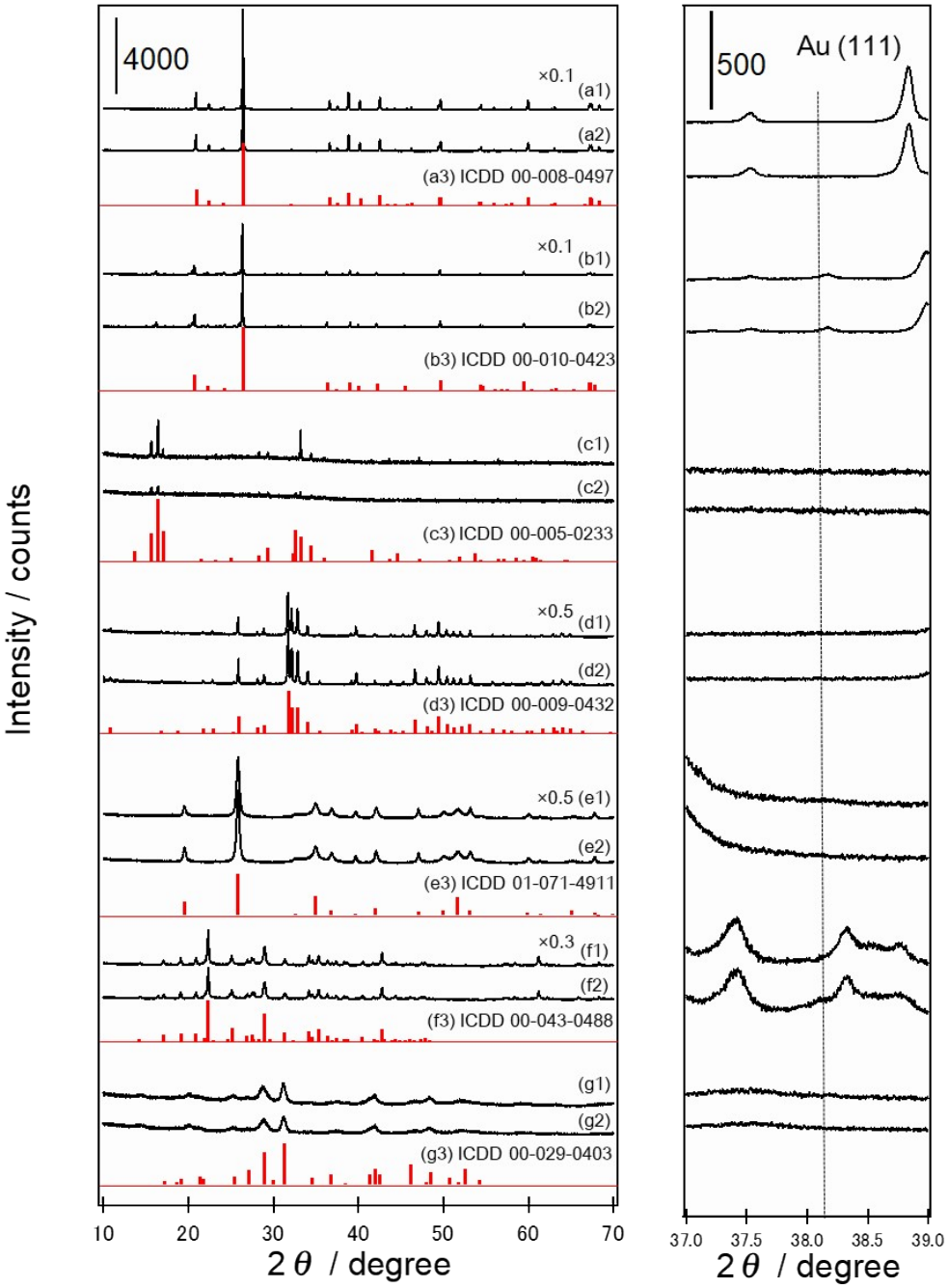

Fig. S2 XRD patterns of metal phosphate-supported Au catalysts on (a1) $GaPO_4$, (b1) $AlPO_4$, (c1) $CrPO_4$, (d1) HAP, (e1) YPO_4, (f1) $Zn_2P_2O_7$, (g1) $CePO_4$, (a2-g2) their supports and (a3-g3) their reference information.

2-3. XRD patterns of metal oxide-supported Au catalysts.

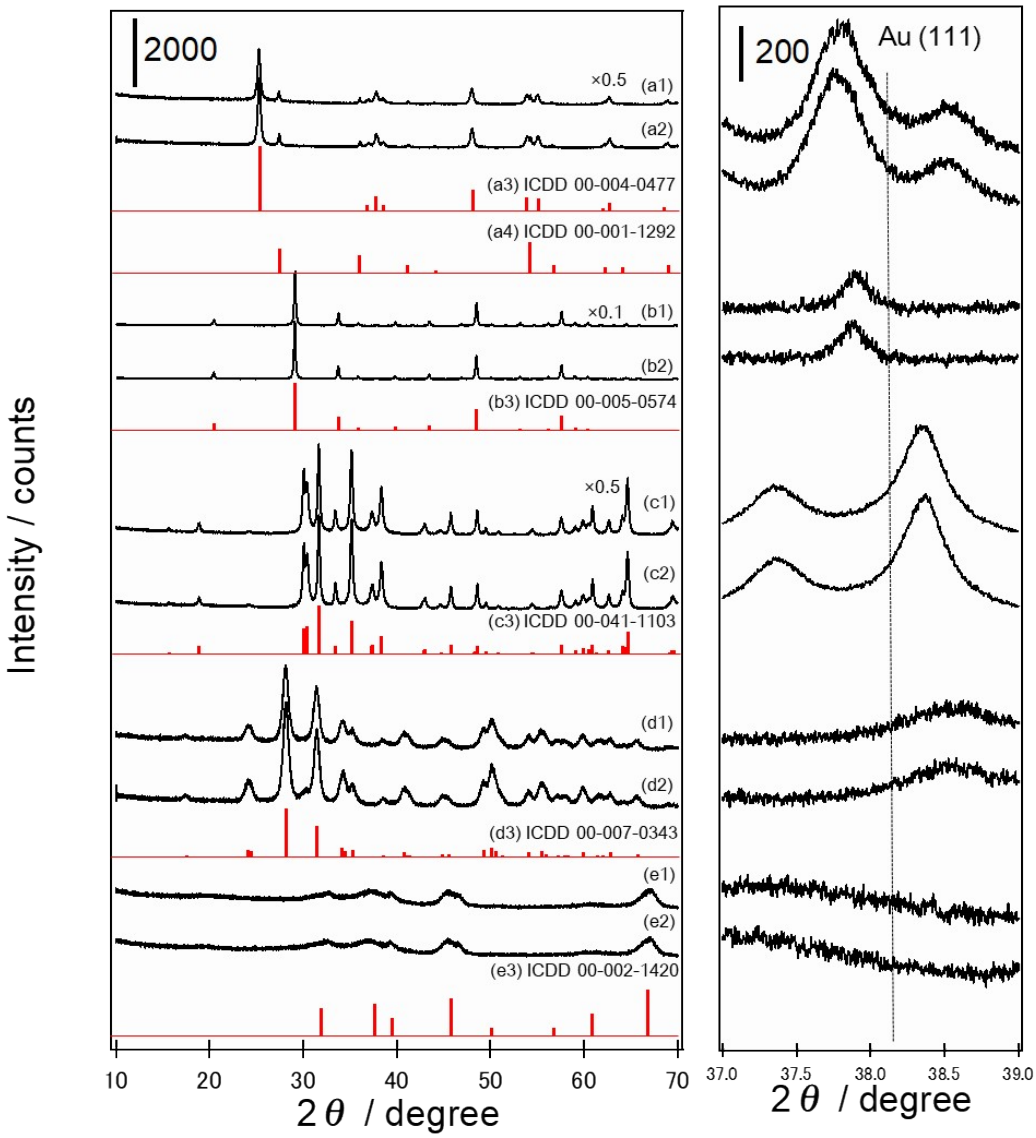

Fig. S3 XRD patterns of metal oxide-supported Au catalysts on (a1) TiO_2, (b1) Y_2O_3, (c1) Ga_2O_3, (d1) ZrO_2, (e1) Al_2O_3, (a2-e2) their supports and (a3-e3) their reference information.

3. HAADF-STEM images and loading amount of metal oxide-supported Au catalysts.

The deposition-precipitation with aq. NaOH (DPNa method) is often used to prepare metal oxide supported Au catalysts. In this study, Au NPs are deposited on TiO_2, Y_2O_3, ZrO_2, and Al_2O_3 with a high loading amount and high dispersion. In contrast, aggregation of Au species was observed on Ga_2O_3. This is probably due to quite a small BET surface area of Ga_2O_3 (8 m^2g^{-1}, data shown in Table S2).

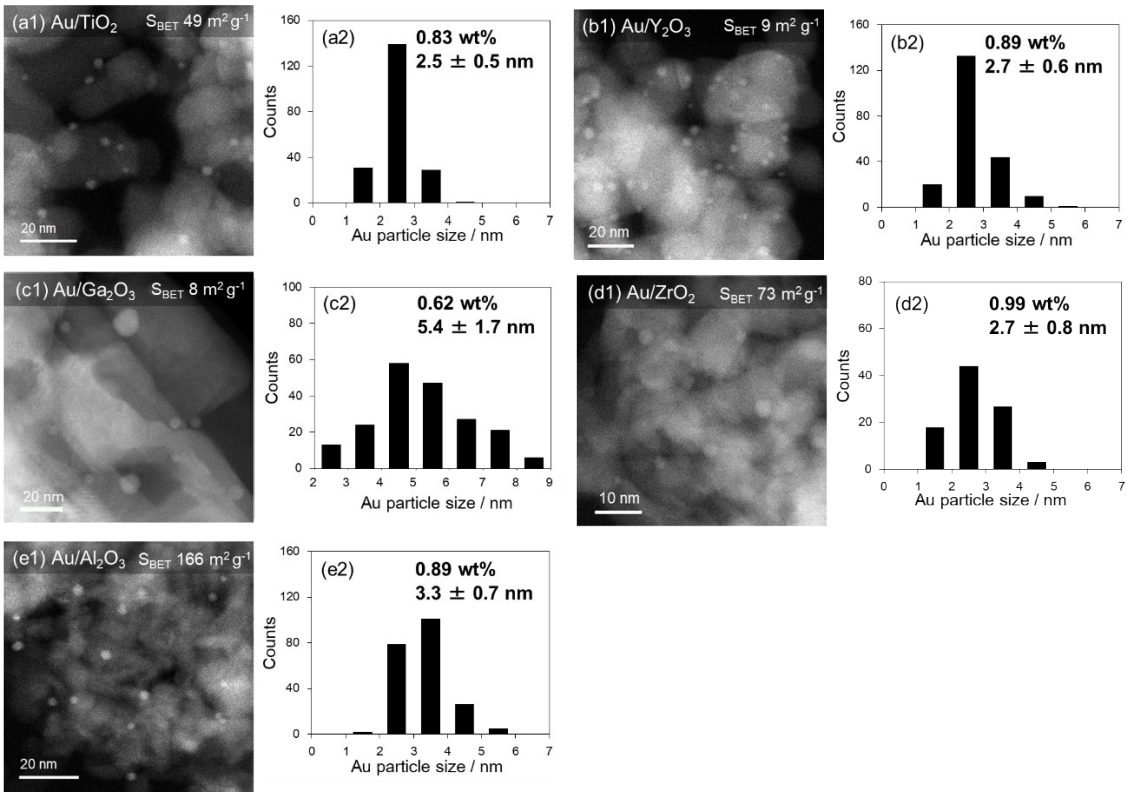

Fig. S4 HAADF-STEM images of metal oxide-supported Au catalysts on (a1) TiO_2, (b1) Y_2O_3, (c1) Ga_2O_3, (d1) ZrO_2, (e1) Al_2O_3 and (a2–e2) particle size distribution histograms and loading amount.

4. Zeta potential of ZrO_2 in aqueous solution as a function of pH.

Zeta potential of ZrO_2 was measured in aqueous solution as a function of pH during deposition-precipitation with aq. NaOH. Fig. S5 shows a comparison of changes in zeta potential of ZrO_2 with and without aqueous $HAuCl_4$ (◆ and ● respectively). The surface potential of ZrO_2 in aq. NaOH solution was negatively shifted by treatment $HAuCl_4$ especially at pH 5-8. This is due to the strong interaction between the anionic gold complex and positively-charged supports.

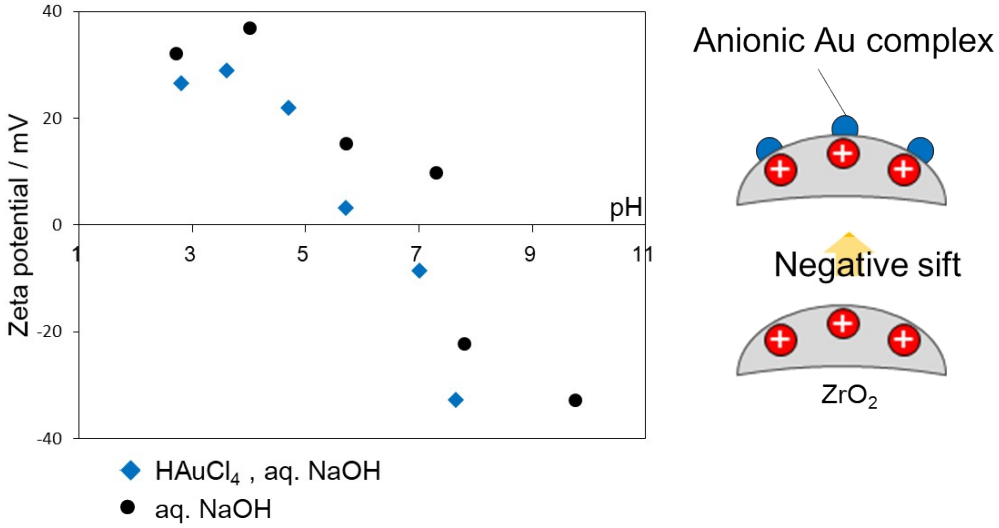

Fig. S5 Zeta potential of ZrP_2O_7 in aqueous solution as a function of pH. The pHs of solutions were adjusted by aq. NaOH. The Zeta potential of ZrO_2 during deposition-precipitation with aq. NaOH as a pH-adjusting reagent is indicated as (▨).

5. XAFS analysis of supported Au catalysts.

5-1. k^3-weighted EXAFS oscillations at the Au L_3-edge of Au/ZrP_2O_7 catalysts before reduction by different preparation method.

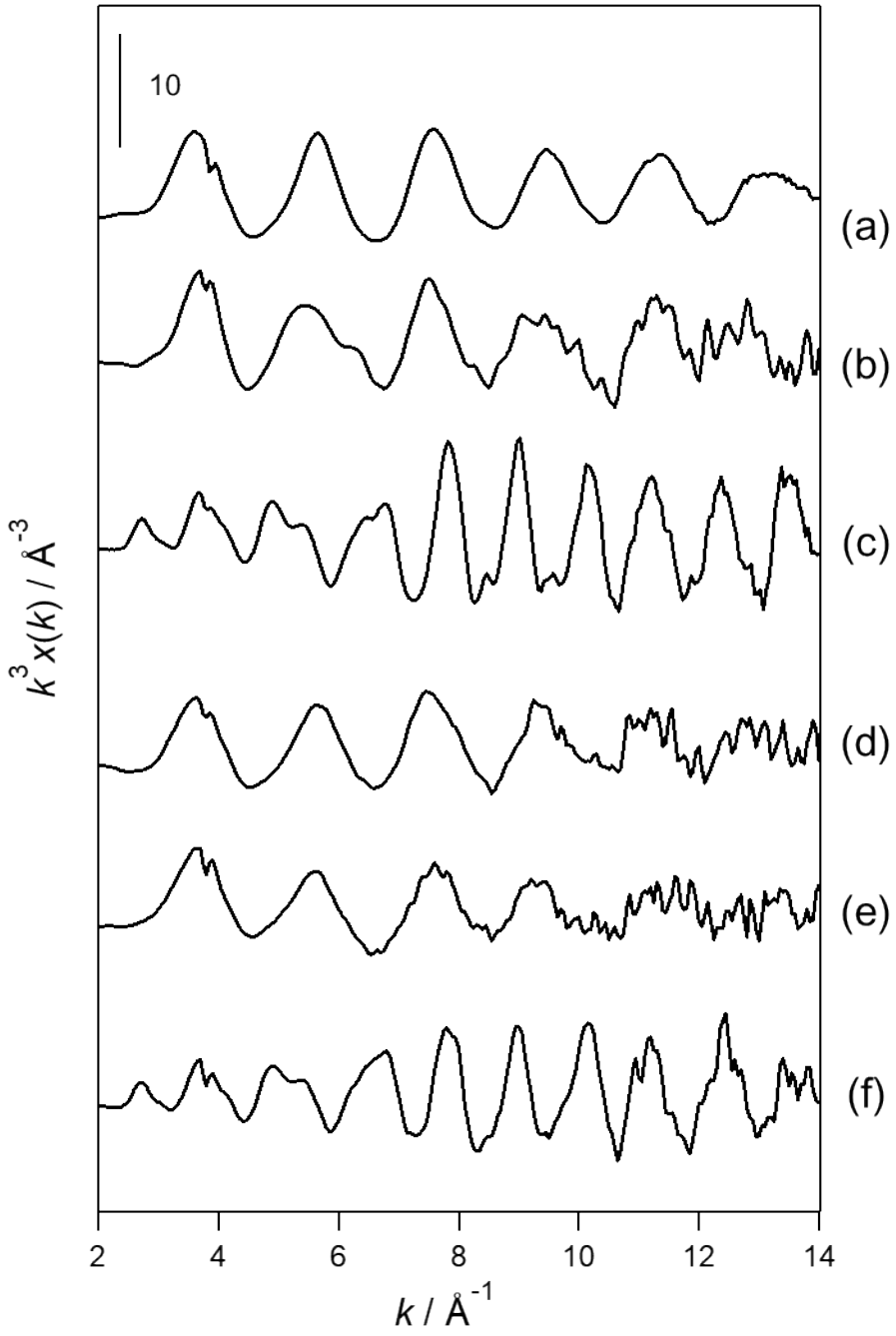

Fig. S6. k^3-weighted EXAFS oscillation at the Au L_3-edge of reference samples (a) Au_2O_3, (b) $Au(en)_2Cl_3$, (c) Au foil and Au/ZrP_2O_7 catalysts before reduction prepared by (d) DPU, (e) DPA, (f) DPen, respectively. Unfortunately, clear spectra of Au/ZrP_2O_7-DPNa was not obtained due to a low Au loading amount.

5-2. Fourier transforms of k^3-weighted EXAFS oscillation at the Au L_3-edge of Au/ZrP_2O_7 catalysts before reduction by different preparation method.

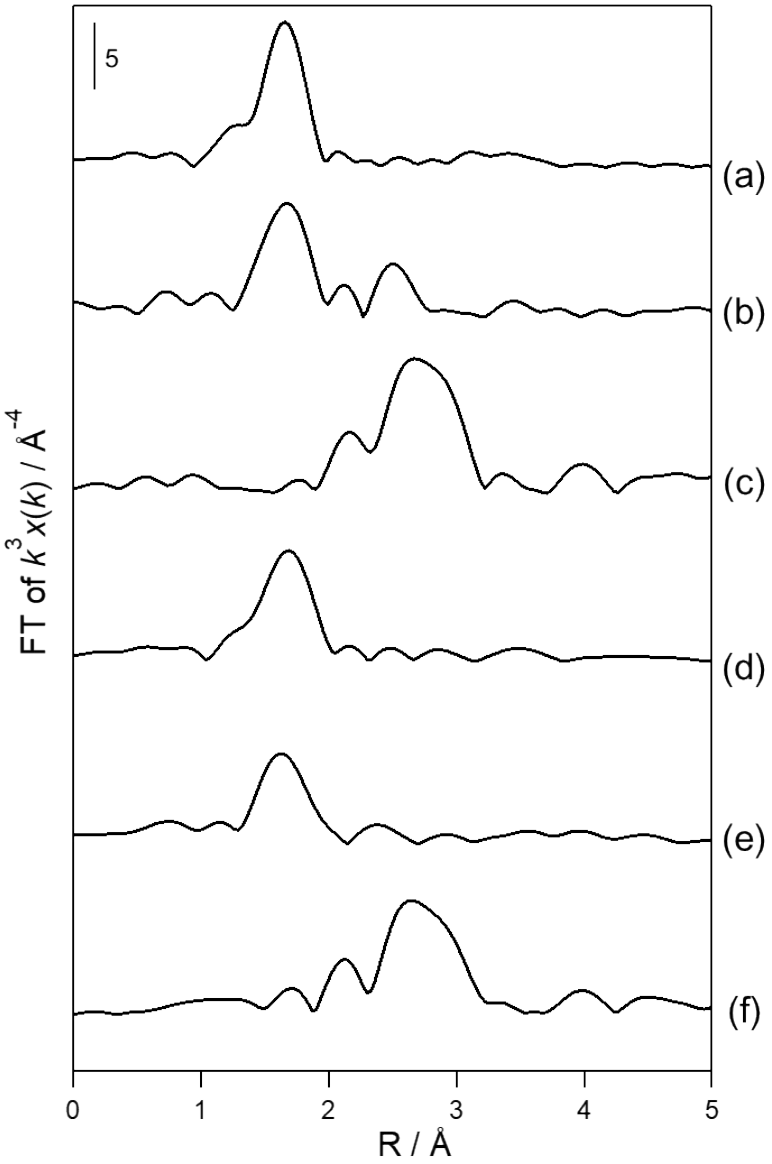

Fig. S7. Fourier transforms of k^3-weighted EXAFS oscillations at the Au L_3-edge of reference samples (a) Au_2O_3, (b) $Au(en)_2Cl_3$, (c) Au foil and Au/ZrP_2O_7 catalysts before reduction prepared by (d) DPU, (e) DPA, (f) DPen, respectively. Unfortunately, clear spectra of Au/ZrP_2O_7-DPNa was not obtained due to a low Au loading amount.

5-3. Au L_3-edge XANES spectra of supported Au catalysts after reduction.

Normalized Au L_3-edge XANES spectra of (a) Au foil and supported Au catalysts on (b) ZrP_2O_7 and (c) ZrO_2 after reduction are shown in Fig. S5. No significant difference in the shape of the spectra of Au/ZrP_2O_7 and Au/ZrO_2 was identified, which suggests that the structure and electronic states of Au supported on metal phosphates and metal oxides are almost same.

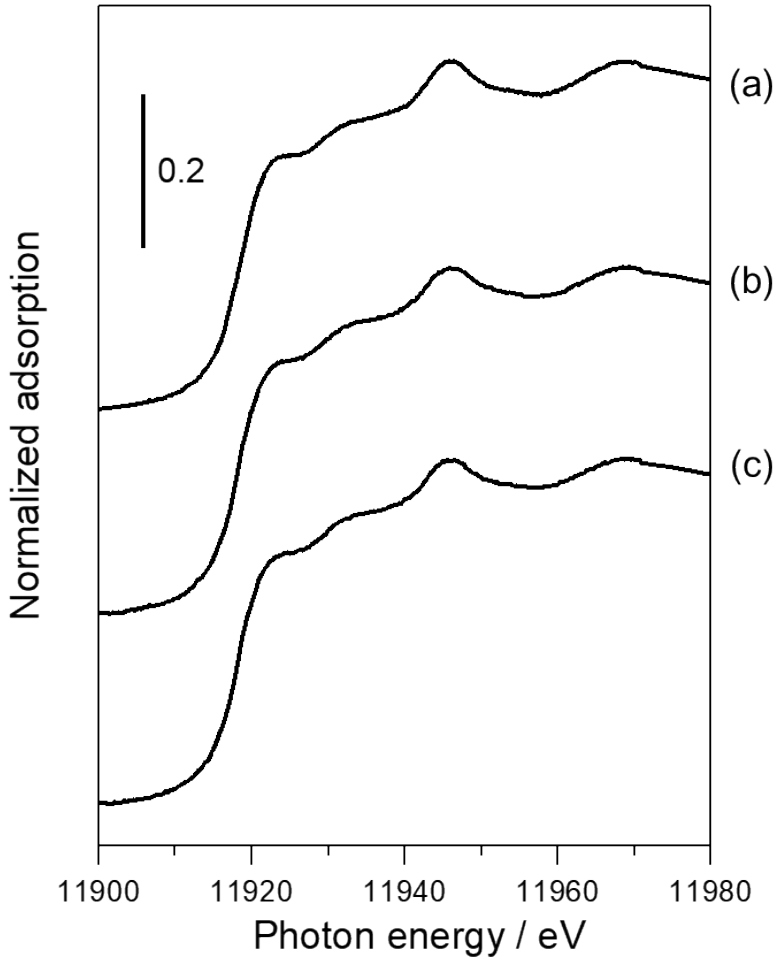

Fig. S8 Au L_3-edge XANES spectra of (a) Au foil and supported Au catalysts on (b) ZrP_2O_7 and (c) ZrO_2 after reduction.

5-4. k^3-weighted EXAFS oscillations at the Au L_3-edge of Au foil and supported Au catalysts after reduction.

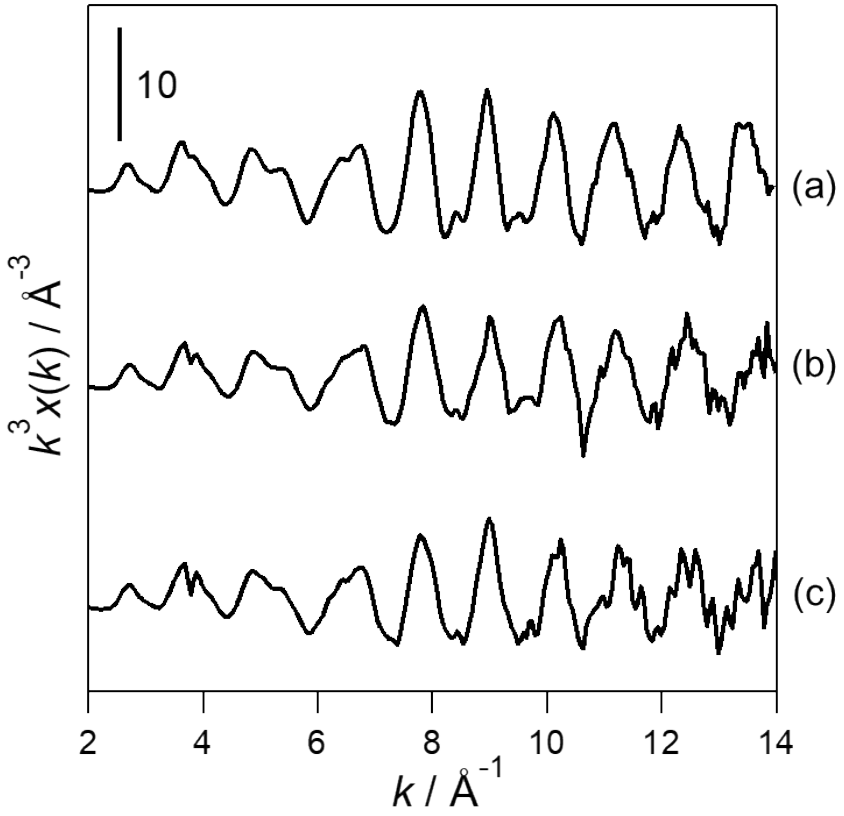

Fig. S9. k^3-weighted EXAFS oscillations at the Au L_3-edge of (a) Au foil and supported Au catalysts on (b) ZrP_2O_7 and (c) ZrO_2 after reduction.

5-5. Fourier transforms of k^3-weighted EXAFS oscillations at the Au L_3-edge of Au foil and supported Au catalysts after reduction.

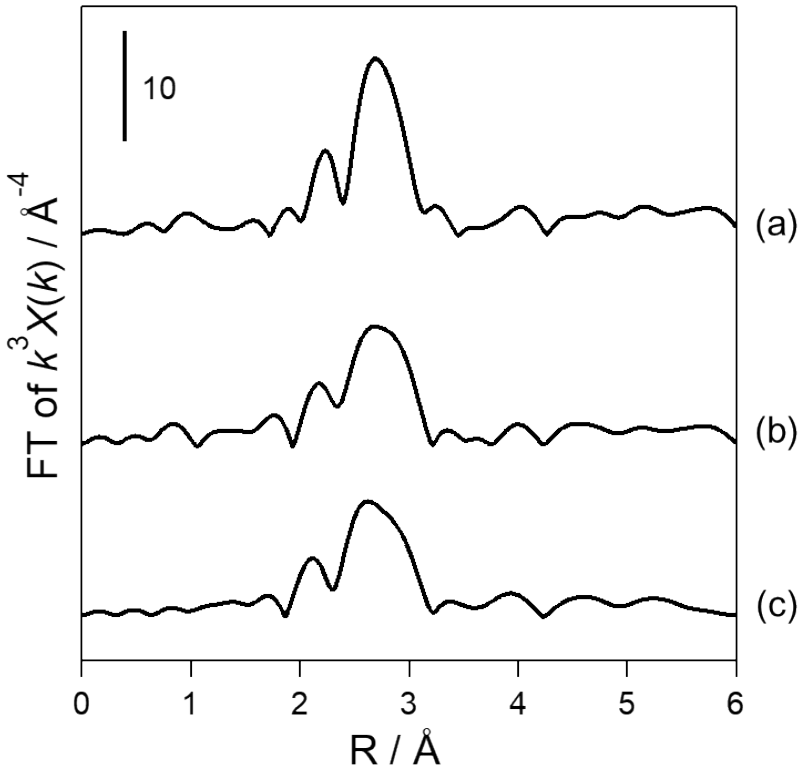

Fig. S10. Fourier transforms of k^3-weighted EXAFS oscillation at the Au L_3-edge of (a) Au foil and supported Au catalysts on (b) ZrP_2O_7 and (c) ZrO_2 after reduction.

6. XP spectra of Au/ZrP_2O_7 before reduction.

The surface element ratio of Au/ZrP_2O_7 prepared by each preparation method before reduction was calculated by XPS measurement. As shown in Table S2, the surface Cl ratio of Au/ZrP_2O_7 prepared by any preparation methods was about 3%. The result indicated that the difference in the dispersion and particle size of Au NPs with each preparation method was not due to the influence of residual Cl, but due to the strong interaction between the Au complex and the support surface.

Table S2 The surface element ratio of Au/ZrP_2O_7 calculated by XPS measurement.

	DPNa	DPU	DPA	DPen
Cl (%)	3	3	3	3
Au (%)	2	15	12	4
Zr (%)	9	11	13	9
P (%)	8	11	13	7
O (%)	78	50	52	74
N (%)	0	11	6	2

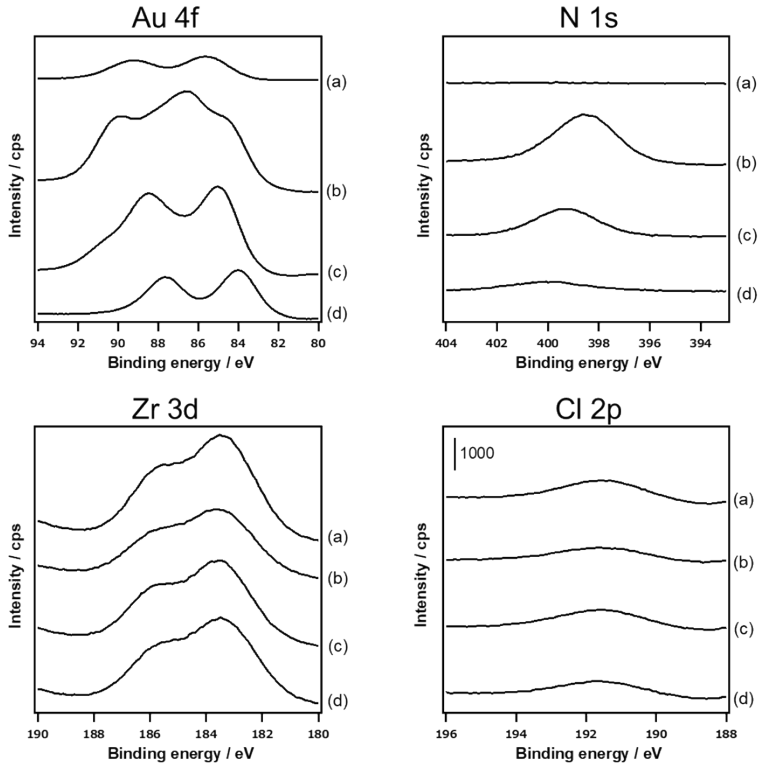

Fig. S11. XP spectra around the Au 4f, N 1s, Zr 3d, Cl 2p states of Au/ZrP_2O_7 prepared by each method (a:DPNa, b:DPU, c:DPA, d:DPen) before reduction.

7. ESI-MS spectra of the Au complex in each preparation method.

To gain the information of gold species in the solution phase before deposition onto supports, we performed ESI-MS of several solutions in the presence of different pH adjusting reagents and Au precursor under both positive and negative mode. As shown in Figure S12, remarkable peaks probably due to anionic $[AuCl_2]^-$ (m/z = 266.90) were identified in the spectra of aqueous $HAuCl_4$ (pH = 3) under negative mode. In contrast, no significant peak was detected under positive mode. In the spectra of solution $HAuCl_4$ treated with NaOH (DPNa method conditions), several peaks with m/z = 200–300 appeared under negative mode, which can be assigned to $[Au(OH)_3]^{2-}$ (m/z = 247.98), $[Au(OH)_2(H_2O)_2]^-$ (m/z = 266.99), and $[Au(OH)_4(H_2O)]^-$ (m/z = 282.99). Under DPen method conditions (pH = 10, the pH adjusted by aq. NaOH), on the other hand, clear peaks probably due to cationic $[Au(C_2H_7N_2)_2]^+$ (m/z = 315.09) were identified in the spectra of aqueous $Au(en)_2Cl_3$ under positive mode. Under DPA method conditions (pH = 11, the pH adjusted by aq. ammonia), a peak can be assigned to $[Au(NH_3)_4]^+$ (m/z = 265.07) or $[Au(NH_3)_2(OH)_2]^+$ (m/z = 265.02) were observed under positive mode. These results suggest that anionic Au complexes were formed in DPNa method, and cationic Au complexes were formed in DPen and DPA method. These results suggest that anionic Au complexes were formed in DPNa method, and cationic Au complexes were formed in DPen and DPA method.

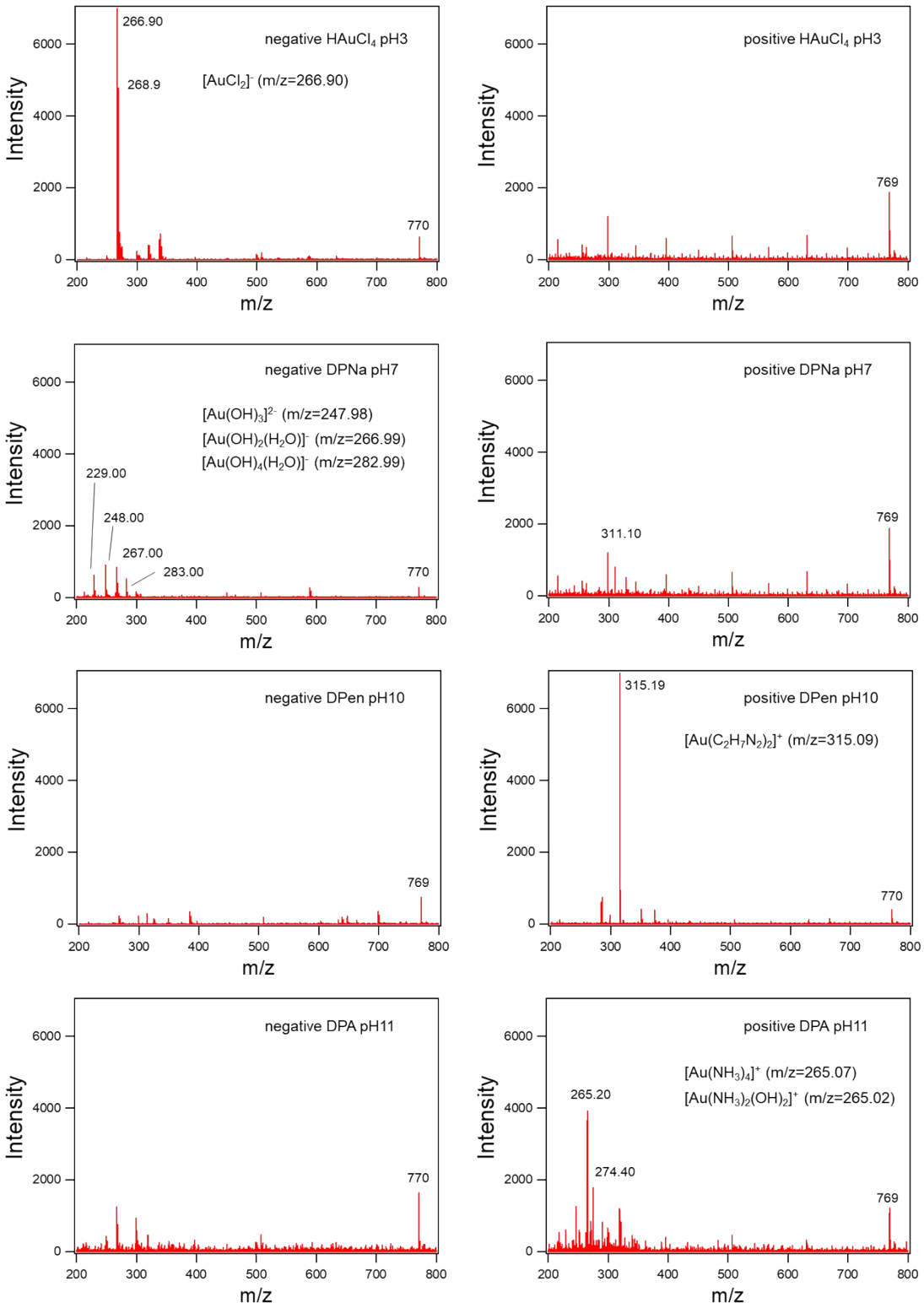

Fig. S12 ESI-MS spectra of Au complex prepared by each method.

8. Hydroamination of phenyl acetylene over metal oxide supported Au catalysts prepared by the DPA method.

Metal oxide supported Au catalysts prepared by the DPNa or DPA were used in the hydroamination of phenyl acetylene to investigate the effect of preparation method (Table S3).

Table S3. Hydroamination of alkyne over a variety of supported Au catalyst [a]

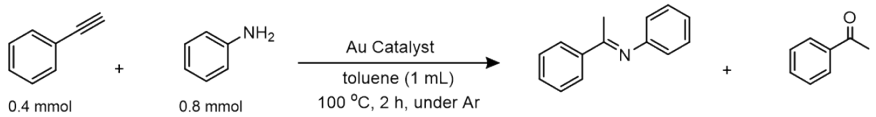

0.4 mmol + 0.8 mmol

Entry	Catalyst	Preparation method	Loading amount / wt% (actual)[b]	Size / nm[c]	Yield (%)[d]		TOF / h^{-1}[e]
					imine	ketone	
1	Au/TiO_2	DPNa	0.83	2.5 ± 0.5	16	1	18
2	Au/Y_2O_3	DPNa	0.89	2.7 ± 0.6	15	2	14
3	Au/Ga_2O_3	DPNa	0.62	5.4 ± 1.7	9	0	16
4	Au/ZrO_2	DPNa	0.99	2.7 ± 0.8	5	1	5
5	Au/Al_2O_3	DPNa	0.89	3.3 ± 0.7	2	0	3
6	Au/TiO_2	DPA	0.86	4.1 ± 1.3	13	3	15
7	Au/Y_2O_3	DPA	0.44	2.2 ± 1.1	1	0	1
8	Au/Ga_2O_3	DPA	0.79	2.8 ± 0.8	12	1	16
9	Au/ZrO_2	DPA	0.98	3.0 ± 2.1	11	0	13
10	Au/Al_2O_3	DPA	0.53	2.4 ± 0.9	2	0	5

[a]Reaction condition : ethynylbenzene (0.4 mmol), aniline (0.8 mmol), Au catalyst (39 mg), toluene (1 mL), 100 °C under Ar. [b]Measured by using atomic absorption spectroscopy (AAS). [c]Measured by TEM image. [d]Determined by ^1H NMR with tetrachloroethane as internal standard. [e]Calculated by Au amount.

9. BET surface areas and base amount of various supported Au catalysts.

Table S4. BET surface areas and base amount of supported Au catalysts

Catalyst	S_{BET} / m^2 g^{-1}	Basicity / μmol g^{-1}
$Au/GaPO_4$	2	0
$Au/AlPO_4$	2	1
Au/ZrP_2O_7	6	2
$Au/CrPO_4$	18	0
Au/HAP	7	4
Au/YPO_4	23	7
$Au/Zn_2P_2O_7$	6	0
$Au/CePO_4$	59	4
Au/TiO_2	49	14
Au/Y_2O_3	9	26
Au/Ga_2O_3	8	0
Au/ZrO_2	73	135
Au/Al_2O_3	166	39

10. Catalytic activities of supported Au catalysts for the hydroamination of alkyne.

Table S5 Catalytic activities of supported Au catalysts for the hydroamination of alkyne.

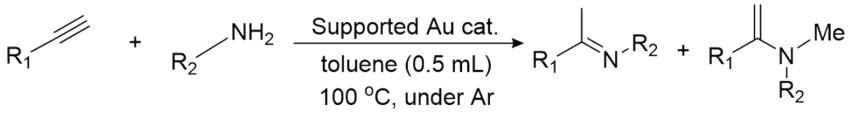

Entry	Alkynes (R_1)	Amines (R_2)	Catalyst	Yield (%)[d]
				imine
1[a]	Ph	Ph	$Au/GaPO_4$	93
2[a]			Au/ZrP_2O_7	82
3[a]			Au/TiO_2	21
4[a]	*p*–Cl–Ph	Ph	$Au/GaPO_4$	81
5[a]			Au/ZrP_2O_7	49
6[a]			Au/TiO_2	15
7[a]	Ph	*p*–Cl–Ph	$Au/GaPO_4$	95
8[a]			Au/ZrP_2O_7	91
9[a]			Au/TiO_2	39
10[b]	^{n}Hex	Ph	$Au/GaPO_4$	49
11[b]			Au/ZrP_2O_7	21
12[b]			Au/TiO_2	4
13[c]	Ph	Ph–NH–CH_3	$Au/GaPO_4$	55
14[c]			Au/ZrP_2O_7	38
15[c]			Au/TiO_2	0

Reaction condition [a]alkyne (0.2 mmol), amine (0.4 mmol), Au catalyst (40 mg, about 1 mol% as Au), toluene (0.5 mL), 100 °C, 4h. [b]alkyne (0.2 mmol), amine (0.4 mmol), Au catalyst (79 mg, about 2 mol% as Au), toluene (0.5 mL), 100 °C, 12h. [c]alkyne (0.2 mmol), amine (0.4 mmol), Au catalyst (39 mg, about 1 mol% as Au), toluene (0.5 mL), 100 °C, 10h. [d]Determined by ^{1}H NMR with tetrachloroethane as internal standard.

11. Hydration of phenylacetylene.

Hydration of phenylacetylene under the condition identical to Table 1 was carried out, and no formation of acetophenone was confirmed (Scheme S1). This suggests that acetophenone is produced by hydrolysis of imine formed by hydroamination of alkyne.

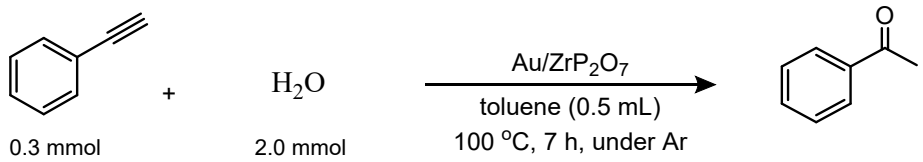

Scheme S1 The hydration of alkyne by Au/ZrP_2O_7. Reaction condition: ethynylbenzene (0.3 mmol), H_2O (2.0 mmol), Au/ZrP_2O_7 (39 mg), toluene (0.5 mL), 100 °C under Ar. The reacton progress was monitored by ^1H NMR with tetrachloroethane as internal standard.

12. Recycling of supported Au catalysts.

12-1. Reusability of Au/ZrP_2O_7 for the hydroamination of alkyne.

Reusability of Au/ZrP_2O_7 catalyst for the hydroamination of alkyne was shown in Fig. S13. Although the conversion rate of alkyne and the yield of imine decrease little by little, the activity did not decrease sharply. By the TEM measurement of the catalyst after the reaction (Fig. S14), it was found that the average particle size increased from 2.8 ± 0.7 nm to 4.2 ± 2.0 nm, and the aggregation of Au NPs maybe caused the decrease in activity of the catalyst.

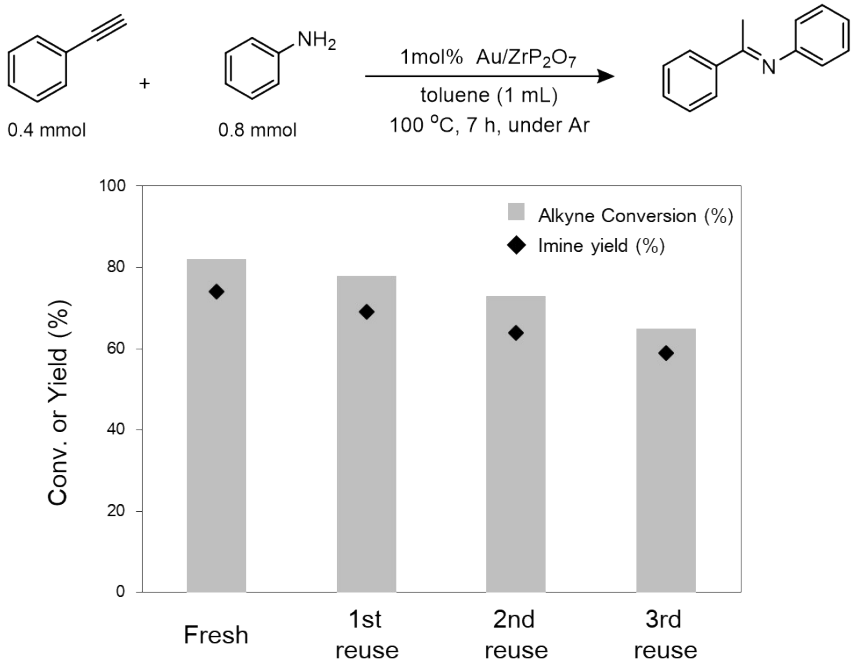

Fig. S13 Reusability of Au/ZrP_2O_7 catalyst for the hydroamination of alkyne. Reaction condition: phenyl acetylene (0.4 mmol), aniline (0.8 mmol), Au/ZrP_2O_7 (1 mol%), toluene (1.0 mL), 100 °C under Ar. Conversion and yield were determined by ^1H NMR with tetrachloroethane as an internal standard.

12-2. HAADF-STEM images of Au/ZrP_2O_7 after reaction.

HAADF-STEM images of Au/ZrP_2O_7 after reaction are shown in Fig. S14. In the fresh catalyst, Au NPs whose mean diameter and standard deviation of Au NPs on ZrP_2O_7 was 3.5 ± 0.9 nm were deposited on ZrP_2O_7 the (Fig. 1-C). However, the average particle size of Au NPs after the reaction was 4.2 ± 2.0 nm, and Au NPs larger than 10 nm were also formed.

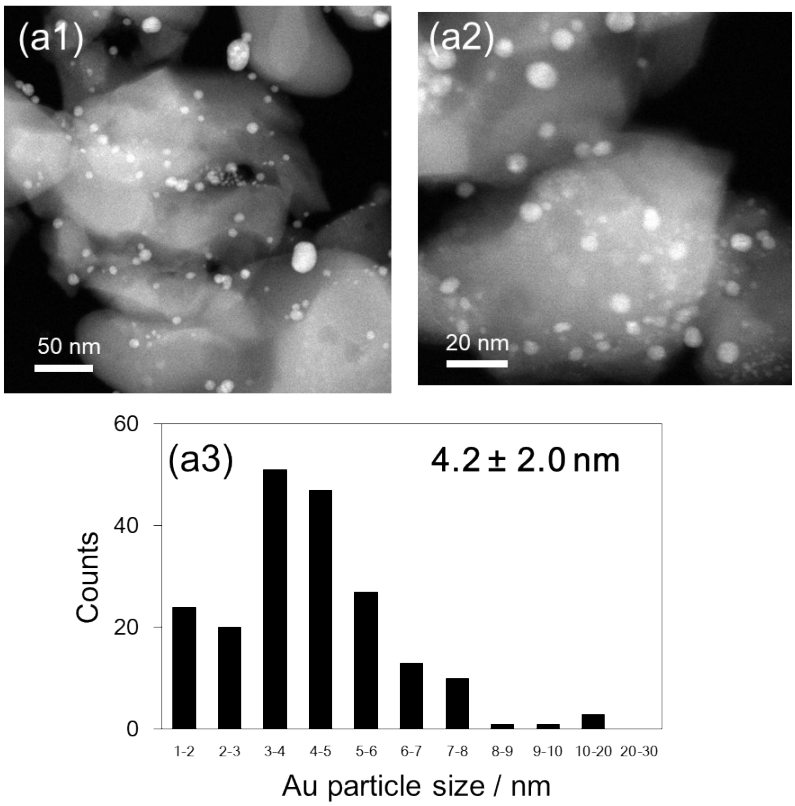

Fig. S14 HAADF-STEM images of Au/ZrP_2O_7 after the reaction (a1,2) and particle size distribution histograms (a3).

12-3. XP spectra around the Au 4f states of Au/ZrP_2O_7 after reaction.

Figure S15 shows the XP spectra around the Au 4f state of Au/ZrP_2O_7 before and after the catalytic run. The peaks due to Au $4f_{7/2}$ and $4f_{5/2}$ did not shift during the reaction, suggesting no change in the electronic state of Au NPs during reaction.

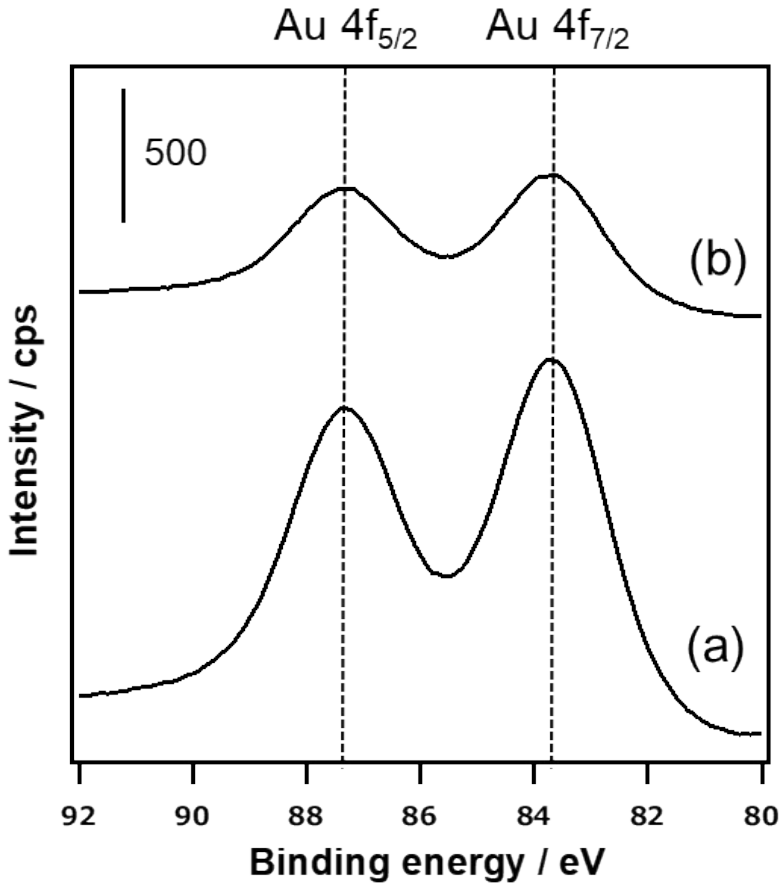

Fig. S15 XP spectra around the Au 4f states of Au/ZrP_2O_7 (a) before reaction (b) after reaction.

13. UV-Vis spectra of the aqueous $HAuCl_4$ in the several conditions

To gain the information of gold complex in solution phase before deposition onto supports, UV-Vis of aqueous $HAuCl_4$ in the presence of aq. NaOH or aq. ammonia were performed. As shown in Figure S16, a remarkable peak due to $AuCl_4^-$ was identified in the spectra of aqueous $HAuCl_4$ (pH = 3). In contrast, no significant peak was detected under DPNa method condition (pH = 7, the pH adjusted by aq. NaOH) or DPA method condition (pH = 11, the pH adjusted by aq. ammonia). Under DPU conditions, unfortunately, a clear spectrum was not obtained due to precipitation formation.

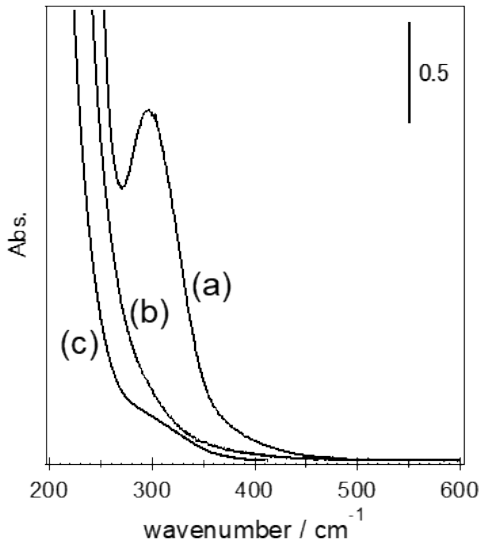

Fig. S16 UV-Vis spectra of the aqueous $HAuCl_4$ in the several conditions. (a) aqueous $HAuCl_4$ (pH = 3) (b) DPNa method condition (pH = 7, the pH adjusted by aq. NaOH) (c) DPA method condition (pH = 11, the pH adjusted by aq. ammonia)